CHEMISTRY
A EUROPEAN JOURNAL

DOI: 10.1002/chem.200800325

A Rigid, Chiral, Dendronized Polymer with a Thermally Stable, Right-Handed Helical Conformation

Afang Zhang,*[a, c] Francisco Rodríguez-Ropero,[b] David Zanuy,[b] Carlos Alemán,*[b] E. W. Meijer,[d] and A. Dieter Schlüter*[a]

Abstract: First- and second-generation dendronized polymethacrylates **PG1** and **PG2** carrying chiral 4-aminoproline-based dendrons were obtained on the half-gram scale in high molar masses (**PG1**: $M_n = 5 \times 10^6\ g\,mol^{-1}$, **PG2**: $M_n = 1 \times 10^6\ g\,mol^{-1}$) by spontaneous (radical) polymerization of the corresponding vinyl macromonomers. NMR spectroscopic studies on **PG2** together with its unprecedented high glass transition temperature ($T_g >$ 200 °C, decomp) and structural parameters provided by atomistic MD simulations show this polymer to be rather rigid. Optical rotation and CD measurements revealed that **PG2** adopts a helical conformation that remains unchanged over wide ranges of temperature and solvent polarity. It is also retained when the polymer is deprotected (and thus positively charged, *de*-**PG2**) at its terminal amino groups, by which the mass and steric demand of the dendrons is reduced by roughly 50 %. Molecular dynamics simulations on models of **PG2** reveal its helical conformation to be right-handed, irrespective of backbone tacticity, and initial results also indicate that *de*-**PG2** retains the right-handedness.

Keywords: dendrons · helical structures · molecular dynamics · polymerization · polymers

Introduction

Chiral helical polymers have received considerable interest recently for mimicking biological helices and developing novel chiral materials.[1] They have been prepared either by achiral polymerization of optically active monomers such as acetylenes,[2] isocyanates,[3] and silanes,[4] or by helix-sense-selective polymerization of achiral monomers (carbodiimides[5] and methacrylates[6]) and chiral monomers (isocyanides[7] and methacrylamides[8]). The former helical polymers are dynamic in solution, and right-handed helices can change into left-handed ones and vice versa under certain conditions, while the helical conformations of the latter are more persistent. Recently, dendronized polymers[9] with polyacetylene backbones were reported by Masuda et al.[10] and Percec et al.[11] to adopt helical conformations with limited thermal stability. In a related recent publication[12] a helical (nondendronized) polyacetylene was reported for which the thermal stability of its helix could be increased significantly by increasing the size of the substituent that followed the chiral center near the backbone.[13] We wondered whether it would be possible to use the "thickening" of polymer chains that occurs in dendronized polymers to render them rigid and, at the same time, chiral with an unprecedented thermally stable helical conformation. We attempted this by polymerizing chiral 4-aminoproline-based second-generation macromonomer **MG2** (Scheme 1), with its rather compact and chiral second-generation dendron, and it was of major interest whether such a monomer would be polymerizable. If so, it was expected that the dendrons would be forced into a tight packing around the backbone which

[a] Prof. Dr. A. Zhang, Prof. Dr. A. D. Schlüter
Institute of Polymers, Department of Materials
ETH Zürich
Wolfgang-Pauli-Straase 10, HCI G525, 8093 Zürich (Switzerland)
Fax: (+41) 44-633-1390
E-mail: azhang@zzu.edu.cn
zhang@mat.ethz.ch
schlueter@mat.ethz.ch

[b] F. Rodríguez-Ropero, D. Zanuy, Prof. Dr. C. Alemán
Departament d'Enginyeria Química
Universitat Politècnica de Catalunya
Diagonal 647, Barcelona 08028 (Spain)
Fax: (+34) 93-4016600
E-mail: carlos.aleman@upc.edu

[c] Prof. Dr. A. Zhang
School of Materials Science and Engineering
Zhengzhou University
Daxue Beilu 75, Zhengzhou 450052 (China)

[d] Prof. Dr. E. W. Meijer
Laboratory of Macromolecular and Organic Chemistry
Eindhoven University of Technology
P.O. Box 513, 5600 MB Eindhoven (The Netherlands)

Supporting information for this article is available on the WWW under http://dx.doi.org/10.1002/chem.200800325 or from the author.

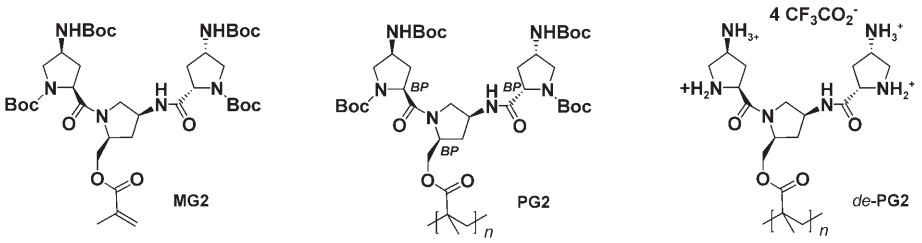

Scheme 1. Chemical structures of second-generation, 4-aminoproline-based, Boc-protected dendronized methacrylate monomer **MG2**, the corresponding polymer **PG2**, and its deprotected derivative *de*-**PG2**. BP stands for branching points, and the number of atoms between them (here 2 and 4) is used in the text as a rough measure of dendron compactness.

should lead to rigidification and helix-sense creation. Here we report the results of the spontaneous polymerization of **MG2** leading to helical dendronized polymer **PG2** together with a spectroscopic and molecular dynamics (MD) simulation analysis on the characteristics of this helix, including stability aspects. A detailed structural model of the helix is also provided.

Results and Discussion

Synthesis: To achieve the goals mentioned above, an ideal dendron should be chiral and compact. Dendrons constructed from 4-aminoproline branching units therefore caught our attention. Taking the atoms between the branching points as a simple measure for compactness,[14] **MG2** should result in a polymer with a very compact dendritic layer that forces consecutive dendrons into register. Because of the chiral nature of the monomer, this could give rise to a biased helix sense of **PG2**. Recently, various such second-generation, diastereomeric dendrons were made available on the gram scale through fully optimized procedures.[15] This includes the dendron contained in **MG2** with its three all-(2*S*,4*S*)-configured branching units (**2a** in Scheme 2), and we therefore decided to use it for the present study. Scheme 2 shows the synthetic sequence to **MG2** and, for comparison purposes, also that to **MG1**. In the first step esters **1a** and **2a** were reduced with $LiBH_4$ to alcohols **1b** and **2b**, which were then esterified with methacryloyl chloride to give the corresponding monomers (**MG1**: 87%; **MG2**: 84%). Both monomers were obtained on a multigram scale as analytically pure materials and characterized by ^1H and ^{13}C NMR spectroscopy, as well as high-resolution mass spectrometry. After careful purification by column chromatography, they were left to stand as highly concentrated DMF solutions at 60°C without addition of any radical initiator, under which conditions even **MG2** started to polymerize spontaneously.[16] After a few hours the solutions had turned solid, and the polymers **PG1** and **PG2** were isolated by column chromatography on silica gel. For comparison, the polymerization of **MG2** was also conducted in the presence of radical initiator 2,2′-azobisisobutyronitrile (AIBN). All polymers were obtained as colorless solids. Their molar masses were determined by gel permeation chromatography (DMF with 1% LiBr as eluent, two-angle light-scattering detection, 45°C), and the results are compiled in Table 1. Polymers **PG1** and **PG2** were obtained with the highest molar masses when polymerization was carried out in concentrated solutions spontaneously (Table 1, entries 1–4). In the presence of 2,2′-azobisisobutyronitrile (AIBN) the molar mass of **PG2** was lower by roughly a factor of two. The molar masses are by far the highest ever obtained for peptidic dendronized polymers even with the less compact amino acids lysine and glutamic acid as repeat units (r.u.s).[17] As is typically observed for dendronized

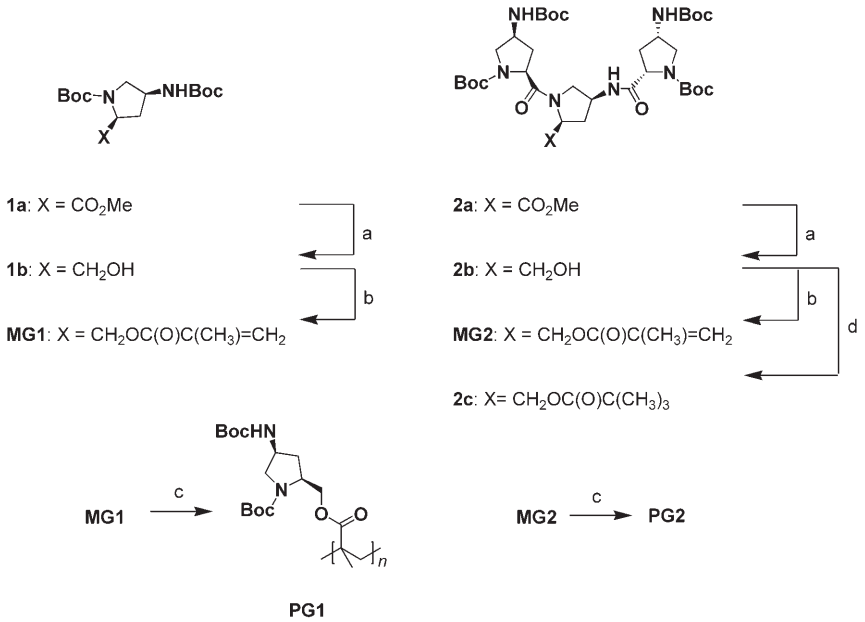

Scheme 2. Synthesis of macromonomers **MG1** and **MG2**, as well as **PG1** and **PG2**. a) $LiBH_4$, THF, −10°C, 12 h (**1b**: 92%, **2b**: 91%); b) MAC, DMAP, NEt_3, THF, 0°C, 12 h (95% and 92% for **MG1** and **MG2**, respectively); c) DMF, 60°C, 12 h; d) trimethylacetyl chloride, NEt_3, DMAP, dichloromethane, 0°C, 6 h (92%). MAC = methacryloyl chloride, DMAP = 4-dimethylaminopyridine.

Table 1. Conditions for and results of polymerization of **MG1** and **MG2**.

Entry	Polymerization conditions[a]			Yield [%]	GPC[b]			T_g [°C]
	Monomer	[Monomer] [M]	Time [h]		$M_n \times 10^{-6}$	DP $\times 10^{-3}$	PDI	
1	**MG1**	1.59	5	80	0.76	2.04	2.80	125
2[c]	**MG1**	2.67	6	52	5.00	13.4	3.66	129
3	**MG2**	0.64	48	50	0.77	0.95	1.94	>200
4	**MG2**	0.79	25	60	1.11	1.37	2.24	>200
5[d]	**MG2**	0.67	24	52	0.38	0.47	2.23	>200

[a] Polymerization carried out at 60 °C in DMF. [b] All GPC measurements were done in DMF at 80 °C. [c] Polymerization in bulk. [d] With 13.8 M AIBN as initiator.

polymers prepared by the macromonomer approach, the average chain lengths of **PG2** were shorter than those of **PG1**.

Polymer rigidity: A first indication of unusual stiffness of **PG2** came from NMR spectroscopy. Although **PG1** and **PG2** with *tert*-butoxycarbonyl (Boc) protecting groups have good solubility in $CDCl_3$ and CD_3OD, only the former polymer gave a reasonable ^1H NMR spectrum at room temperature in which all expected signals were visible (Figure 1a, top). For the latter, only a broad signal for the peripheral Boc groups was recorded and most of the other signals were absent (Figure 1a, bottom).[18] The same phenomenon was observed for the ^{13}C NMR spectrum of **PG2**, in which again practically all signals were absent, except for those of the Boc groups (Figure 1b, top). The solid-state CPMAS ^{13}C NMR spectrum of **PG2** showed all expected signals (Figure 1b, bottom). It seems that the reduced mobility of the magnetic nuclei due to the high rigidity of **PG2** is responsible for these effects, which were not encountered to this extent with our other dendronized polymers. Differential scanning calorimetry (DSC) measurements gave T_g values for **PG1** and **PG2** of 129 and above 200 °C (beyond decomposition), respectively, which are the highest so far observed for (less compact) dendronized polymers. Typically, T_g values are in the range of 55–80 °C.[14c] Compared to parent poly(methyl methacrylate), PMMA ($T_g = 105$ °C), the T_g of **PG2** is at least 95 °C higher, which indicates an increase in rigidity, though the glass transition is not only determined by chain stiffness. Due to the low resolution of the proton spectrum of **PG2**, the backbone tacticity was estimated by using its analogue *de*-**PG2**. In contrast to PMMAs from conventional radical polymerization in DMF, the backbones of which are dominated by syndiotactic units (ca. 62%),[19] *de*-**PG2** contains mostly heterotactic (ca. 63%) and a smaller amount of syndiotactic units (ca. 32%, see Figure S2 in the Supporting Information).

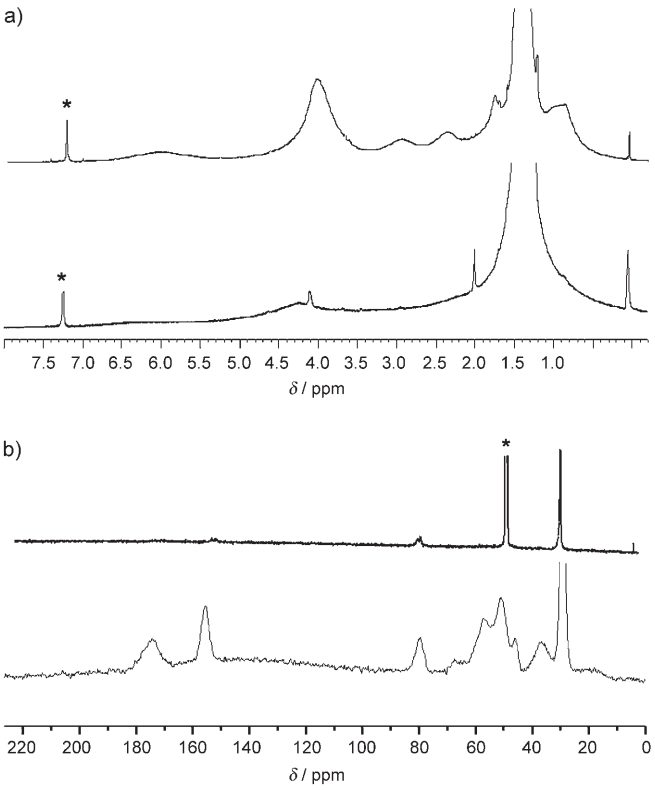

Figure 1. a) ^1H NMR spectra of **PG1** (top) and **PG2** (bottom) in $CDCl_3$ and b) ^{13}C NMR spectra of **PG2** in CD_3OD (top) and in the solid state (bottom) at room temperature. Solvent peaks are marked with asterisks.

It is noteworthy that the ester bonds of **PG2** through which the dendrons are attached to the backbone cannot be easily saponified. Treatment with lithium or sodium hydroxide in refluxing MeOH for 24 h left this polymer completely unchanged, whereas other less compact dendronized polymers (of even higher generation) can be efficiently dedendronized under these conditions.[20] This is an indication of the compactness of the dendritic layer of **PG2**.

Finally, MD simulations in both chloroform and methanol solutions of a model polymer chain consisting of 20 repeat units were performed to investigate the rigidity of **PG2** at the atomistic level. Simulations were performed with explicit solvent molecules and a helical conformation compatible with available experimental data, which was derived from a systematic conformational search (see below). The end-to-end distance remained unchanged at (46.83 ± 0.26) and (46.32 ± 0.45) Å in chloroform and methanol, respectively, during the whole simulation time range of 50 ns (Figure 2). The high stiffness of **PG2** was also supported by the constant cross-sectional diameter (average values: 29.16 ± 0.30 and 29.10 ± 0.44 Å in chloroform and methanol, respectively). Consistently, the temporal evolution of this property shows that no significant fluctuation occurred along the trajectories (Figure 2).

Secondary structure and helix conformation: The secondary structures of the polymers were investigated by optical rotation (OR) and circular dichroism (CD) spectroscopic meas-

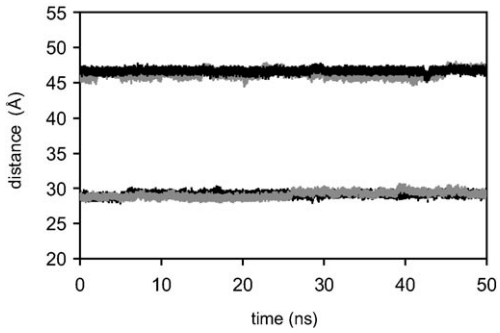

Figure 2. Time-dependent evolution of the end-to-end distance (upper data set) and the cross-sectional diameter (lower data set) in chloroform (black lines) and methanol (gray lines) solution. The lines representing the two environments overlap.

urements (Table 2, Figure 3). The OR measurements were performed with protected polymers **PG1** and **PG2**, whereas the CD spectra were additionally recorded also for both the deprotected and thus positively charged *de*-**PG1** and *de*-**PG2**. The OR of **PG1** was practically identical to that of **MG1**, whereas for **PG2** it was slightly less intense compared to that of **MG2**, irrespective of whether CH_3OH or $CHCl_3$

Table 2. Specific rotations of **MG1**, **MG2**, **PG1**, and **PG2**.[a]

Entry	c [g dL^{-1}]	$[\alpha]_D^{25}$	
		MeOH	$CHCl_3$
MG1	1.48	−30.3	–
PG1	1.25	−31.6	–
MG2	1.13 (1.02[b])	−37.1	−52.6
PG2	0.95 (1.14[b])	−22.3	−38.9

[a] All measurements were done at 25 °C in MeOH in a 1 dm cuvette. [b] In chloroform.

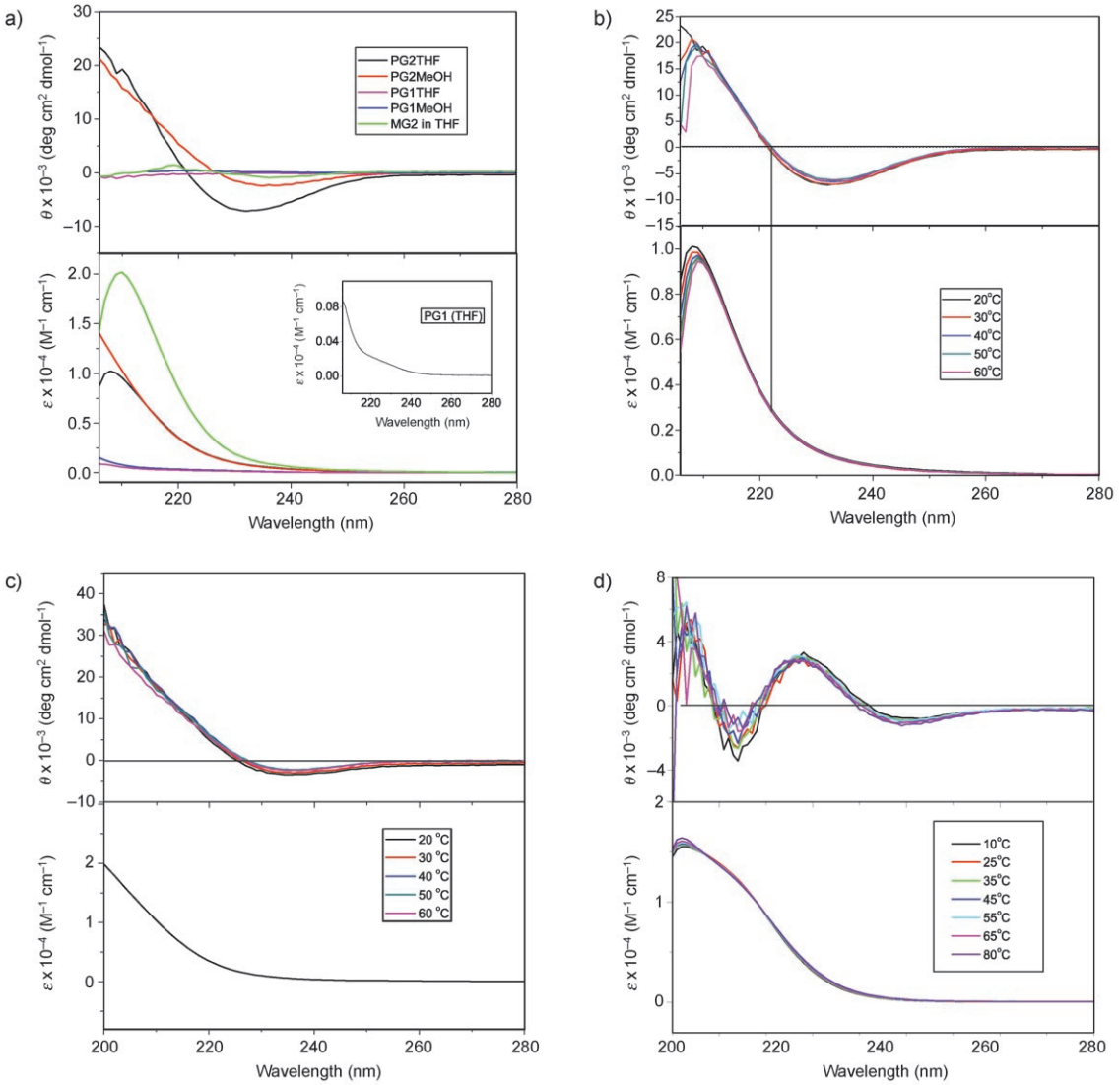

Figure 3. CD (top) and UV spectra (bottom) of a) **MG2** in THF and polymers **PG1** and **PG2** in MeOH and THF at room temperature (inset: UV spectrum of **PG1** in THF), b) **PG2** in THF, c) **PG2** in MeOH, and d) *de*-**PG2** in water at different temperatures.

was used as solvent. This decrease suggests a different secondary structure for the polymer compared to the monomer and is most likely due to restricted conformational freedom in **PG2**.[21] In other words, **PG1** does not adopt an ordered secondary structure, while **PG2** may do so, though the difference in OR between **MG2** and **PG2** is rather small. Such small differences were interpreted by Masuda et al.[12] in terms of high rigidity of the polymer backbone.

Figure 3 summarizes the results of all CD and UV spectroscopic measurements performed with **PG1**, **PG2**, and *de*-**PG2** in different solvents and at different temperatures. Figure 3a shows the normalized CD spectra of **PG1** and **PG2** in MeOH and THF. The former did not exhibit a significant absorption in the range of $\lambda = 200$–260 nm, whereas the latter has a negative Cotton effect at $\lambda = 232$ nm. This is a strong indication that **PG2**, but not **PG1**, adopts an ordered secondary structure. The CD spectrum of **MG2** in THF was also recorded for comparison and showed only a weak negative signal at 237 nm (Figure 3a), which again suggests that **PG2** adopts an ordered structure in solution. The Cotton effect of **PG2** was stronger in THF than in MeOH. Figure 3b and c show the temperature-dependent CD and UV spectra of **PG2** in THF and MeOH, respectively. In the temperature range of 20–60 °C, they turned out to be practically superimposable, indicative of a fully retained secondary structure under these conditions. Figure 3d shows the behavior of *de*-**PG2** in water at pH 4 in the temperature range of 10–80 °C. The appearance of its CD and UV spectra differs from the above because of the different chromophore. Despite the considerable loss of mass associated with deprotection, the secondary structure is basically retained, though a somewhat more pronounced temperature dependence is observed as compared with protected congener **PG2**.

These results point towards a stable and chiral secondary structure of **PG2**, which even seems to be largely maintained in the deprotected form. The nature of the secondary structure was addressed by computations combining quantum chemical methods and MD simulations (see Experimental Section) based on isotactic and heterotactic model polymers with 20 repeat units.[22] Initially, the more favorable arrangements of the model compound **2c** (Scheme 2), resembling a large part of the polymer repeat unit, were examined by exploring its potential-energy hypersurface. More specifically, a rigorous multidimensional conformational analysis was performed by considering that three minima are expected for each flexible dihedral angle involved in the fragment of **2c** containing four aminoproline residues. Twenty-seven possible structures were considered as starting points for complete geometry optimization at the HF/3-21G level,[23] and the 18 minima of lower energy were reoptimized at the HF/6-31G(d) level;[24] the remaining HF/3-21G minima were separated from the lowest-energy minimum by more than 10 kcal mol^{-1}. Finally, single-point calculations at the B3LYP/6-31G(d) level[25] were carried out on the resulting HF/6-31G(d) geometries to obtain reliable energy estimates.

The two most stable conformations of **2c** were considered in a systematic study devoted to building sterically accessible helical models. For this purpose, the backbone dihedral angles of the dendronized methacrylate repeat unit, hereafter denoted χ_1 and χ_2, were varied systematically in steps of 30° within an isotactic model system of **PG2** consisting of 20 repeat units, which were kept with identical conformation. The structures without apparent steric contacts were subjected to energy minimization with the Amber force field.[26] Surprisingly, 80 helical conformations were able to retain their regularity and homogeneity, that is, similar (± 20°) values of χ_1 and χ_2 for the 20 repeat units. Next, the 80 structures were submitted to 0.5 ns of MD at 298 K in the absence of environment. Only eight models maintained the secondary structure, and the helical conformation of the remaining 72 models was rapidly lost owing to thermal vibrations. After this, a NVT-MD in chloroform solution was run for 6 ns for each of the eight structures. These simulations provided two models with regular and homogeneous secondary structure and, in addition, similar energies. Finally, 6 ns NVT-MD simulations in methanol solution were performed for these two structures. Although the regularity was maintained again and their internal energies were very similar in the two cases, the solute–solvent interactions were significantly more favorable for one of the two helical models.

It consists of a right-handed helix with average backbone dihedral angles of $\chi_1 = (-159.5 \pm 2.8)$° and $\chi_2 = (-52.2 \pm 2.1)$° (Figure 4a). The characteristic helical parameters derived for this structure considering an idealized system formed by identical repeat units (Figure 4a) are 2.65 repeat units per turn, 0.71 Å internal radius, and 2.12 Å rise per repeat unit. This structure not only remains stable but also is very rigid in solution in both chloroform and methanol (Figure 2). These unique properties should be attributed not only to the size of the dendron but also to the hydrogen-bonding network detected in the secondary structure, which extends along the whole polymer chain. Thus, the NH groups of the 4-aminoproline residues form this kind of interaction with the amide oxygen atoms of either the neighboring repeat unit (Figure 4b, right) or the same repeat unit (Figure 4b, left), which enhances the stability and stiffness of the helical conformation.

To ascertain whether this helical model is only valid for isotactic **PG2** or does not depend on the backbone tacticity, a complementary study was performed on syndiotactic and heterotactic models for a polymer chain of 20 repeat units. Table 3 lists the 16 sequences used for such study, where A and B refer to repeat units that differ in the configuration in the chiral backbone atom. Isotactic, syndiotactic, and heterotactic models were analyzed. Initially, the helix found for the isotactic A_{20} model was imposed in the other 15 sequences. After energy minimization, a regular and homogeneous helical conformation was retained in all cases. Next, each minimized structure was subjected to 10 ns of NVT-MD simulation in chloroform solution, equilibration, and thermalization of the simulation box (see Experimental Section for protocol).

The helical structure was stable for all the investigated sequences, as evidenced by the small values of the averaged

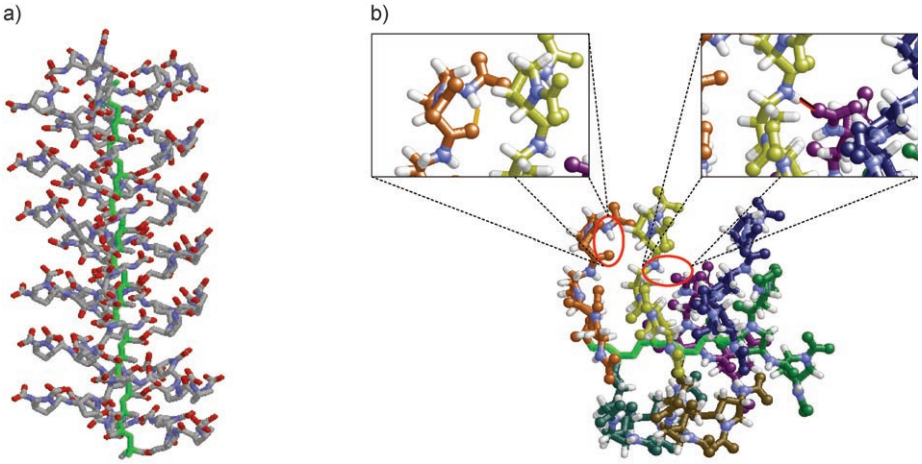

Figure 4. a) Axial projection of the right-handed helical model of **PG2**. *tert*-Butyl groups and hydrogen atoms have been removed for clarity. The backbone is represented by a solid green line. b) Details of the N–H···O= C hydrogen-bonding network detected in the helical secondary structure. The magnified view on the right shows the hydrogen bond (red line) between different r.u.s, and that on the left the hydrogen bond (yellow line) between groups of the same r.u.

(over the whole simulation) root-mean-square deviations ($RMSD_{Av}$) of the backbone, which were calculated relative to the right-handed helix proposed for model A_{20}. Thus, the $RMSD_{Av}$ values (Table 3) were smaller than 2 Å in all cases, independent of backbone tacticity. Furthermore, The $RMSD_{Av}$ value obtained for the syndiotactic sequence $(A\text{-}B)_{10}$ is extremely low ((0.744 ± 0.148) Å), whereas the values for the sequences formed by short blocks of A and B repeat units are also notably low (≈1 Å).

Figure 5a compares the temporal evolution of the backbone RMSD for selected models: syndiotactic $(A\text{-}B)_{10}$, isotatic B_{20} and, heterotactic $A\text{-}(A\text{-}B)_2\text{-}A_3\text{-}B_4\text{-}A_3\text{-}B\text{-}A_4$ and $A_8\text{-}B_4\text{-}A_8$. Although in some cases, for example, $A\text{-}(A\text{-}B)_2\text{-}A_3\text{-}B_4\text{-}A_3\text{-}B\text{-}A_4$, minor conformational rearrangement occurs after 4–5 ns, in general the RMSD converges after a few hundred picoseconds. Practically identical behavior was found for the re-

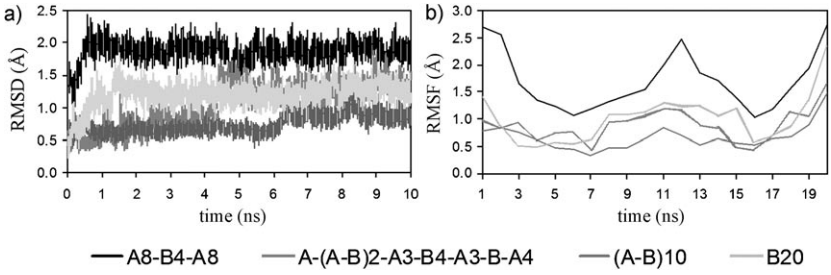

Figure 5. a) Evolution of the backbone RMSD for four selected models of dendronized polymer **PG2** with respect to the right-handed helix proposed for the isotactic model A_{20}. b) RMSF calculated for the 20 r.u.s considered in the four selected models. Graphics for the other 11 models investigated (see Table 3) are provided in the Supporting Information.

Table 3. Average values of the backbone root-mean-square deviation ($RMSD_{Av}$)[a] calculated with respect to the idealized helical model proposed after a detailed conformational search on an isotactic model, backbone dihedral angles (χ_1, χ_2),[a] cross-sectional diameter (D),[a] end-to-end distance (d_{e-e}),[a] internal energy of the helix[b] relative to the most stable model (ΔE_{den}), and potential energy of the whole simulated system[b] (dendronized polymer and explicit solvent molecules) relative to the most stable system (ΔE_{den+s}).

Model[c]	$RMSD_{Av}$ [Å]	χ_1, χ_2 [°]	D [Å]	d_{e-e} [Å]	ΔE_{den} [kcal mol^{-1} (r.u.)$^{-1}$]	ΔE_{den+s} [kcal mol^{-1} (r.u.)$^{-1}$]
$A_8\text{-}B_4\text{-}A_8$	1.875 ± 0.288	−169.0 ± 1.9, −110.8 ± 8.1	30.11 ± 0.23	37.88 ± 0.80	2.2	−0.6
$A_7\text{-}B\text{-}A_4\text{-}(B\text{-}A)_2\text{-}A_2B\text{-}A$	1.368 ± 0.256	−165.2 ± 2.0, −67.9 ± 2.2	30.33 ± 0.20	45.12 ± 0.51	0.3	−2.5
$A_2\text{-}B\text{-}A_6\text{-}B\text{-}A\text{-}B\text{-}A_3B\text{-}A_4$	1.676 ± 0.512	−166.6 ± 2.8, −90.5 ± 7.3	30.05 ± 0.29	40.16 ± 1.45	0.0	0.0
$A_2\text{-}B\text{-}A_6\text{-}B_3\text{-}A_3\text{-}B\text{-}A_4$	1.154 ± 0.188	−173.6 ± 3.3, −94.0 ± 1.7	30.42 ± 0.34	45.93 ± 0.50	2.8	−0.2
$A\text{-}(A\text{-}B)_2\text{-}A_4\text{-}B_3\text{-}A_3\text{-}B\text{-}A_4$	1.734 ± 0.215	−168.1 ± 1.9, −67.8 ± 1.5	30.43 ± 0.26	44.51 ± 0.32	2.4	−1.9
$A\text{-}(A\text{-}B)_2\text{-}A_3\text{-}B_4\text{-}A_3\text{-}B\text{-}A_4$	1.049 ± 0.343	−163.3 ± 2.3, −70.6 ± 1.4	29.84 ± 0.27	45.74 ± 0.50	0.8	−1.9
$A_2\text{-}B_3\text{-}A_3\text{-}B_4\text{-}A_3\text{-}B\text{-}A_4$	1.457 ± 0.232	−169.7 ± 2.8, −67.5 ± 1.4	29.18 ± 0.31	41.23 ± 0.69	3.1	−2.1
$A_2\text{-}B_3\text{-}A_2\text{-}B_5\text{-}A_3\text{-}B\text{-}A_4$	1.037 ± 0.142	−167.5 ± 2.5, −67.8 ± 1.5	29.44 ± 0.20	44.67 ± 0.41	2.6	−2.5
$A_2\text{-}B_3\text{-}A_2\text{-}B_6\text{-}A_2\text{-}B_2\text{-}A_3$	1.009 ± 0.186	−161.1 ± 2.5, −70.2 ± 1.6	29.56 ± 0.21	42.85 ± 0.89	3.2	2.8
$A_2\text{-}B_3\text{-}A_2\text{-}B_6\text{-}A_2\text{-}B_2\text{-}A_2\text{-}B$	0.888 ± 0.123	−163.5 ± 2.1, −68.1 ± 1.4	29.67 ± 0.48	44.14 ± 0.45	1.3	−0.2
$B\text{-}A\text{-}B_3\text{-}A_2\text{-}B_6\text{-}A_2\text{-}B_2\text{-}A_2\text{-}B$	1.131 ± 0.142	−164.8 ± 2.4, −68.7 ± 1.5	30.53 ± 0.36	44.08 ± 0.76	3.7	−1.9
A_{20}	–[d]	−159.5 ± 2.8, −52.2 ± 2.1	29.35 ± 0.32	46.83 ± 0.26	1.3	−1.4
B_{20}	1.196 ± 0.190	−167.6 ± 2.1, −64.6 ± 1.8	29.41 ± 0.39	45.17 ± 0.31	1.7	−1.6
$(A\text{-}B)_{10}$	0.744 ± 0.148	−161.5 ± 2.1, −57.8 ± 1.3	29.83 ± 0.27	46.03 ± 0.42	0.1	−2.1
$(A_3\text{-}B_3)_3\text{-}A_2$	1.097 ± 0.229	−163.9 ± 2.5, −67.3 ± 2.2	30.77 ± 0.58	45.01 ± 0.79	3.0	−1.3
$(A_5\text{-}B_5)_2$	1.946 ± 0.229	−167.4 ± 2.4, −72.7 ± 2.0	29.53 ± 0.25	45.20 ± 0.70	3.2	0.5

[a] Averaged over the whole simulation. [b] Averaged over the last 50 recorded snapshots. [c] A and B refer to repeat units that differ in the configuration in the chiral backbone atom. [d] Used to derive the idealized helical model of A_{20}, which was used as reference.

maining 11 models (see the Supporting Information). Thus, for each model the RMSD remains close to the average value (Table 3) for the whole simulation, that is, the stability of the proposed helical model is remarkably high and does not depend on backbone tacticity. Figure 5b displays the backbone root-mean-square fluctuation (RMSF) of the individual repeat unit averaged over the whole simulation for the four models selected above. Although, in general, no significant fluctuation was found for the 20 repeat units, the distortions were larger for the model A_8-B_4-A_8. Inspection of the RMSF obtained for this model clearly indicates that the main distortions are located in the short B block and the extremes of the molecule. In contrast, the low and uniform RMSF values for all 20 repeat units of the A-$(A\text{-}B)_2$-A_3-B_4-A_3-B-A_4, B_{20}, and $(A\text{-}B)_{10}$ models, especially for the last-named, evidences a remarkable conservation of the right-handed helix. These results combined with those provided in the Supporting Information clearly demonstrate that the helical structure proposed for the isotactic polymer does not depend on backbone tacticity; this structural motif is also compatible with syndiotactic and heterotactic systems. However, both RMSD and RMSF profiles suggest that such a helical conformation is particularly stable when the A and B repeat units alternate frequently, that is, ideally in a syndiotactic arrangement.

Table 3 includes the average values of the structural parameters determined for the 16 sequences examined: diameter of the helix D and end-to-end distance d_{e-e}. These parameters are in agreement with those obtained for the isotactic model used in the conformational search strategy. Furthermore, the very small standard deviations of the resulting values in all cases indicate that the reduced mobility and high rigidity found for **PG2** is also independent of backbone tacticity.

On the other hand, the decrease in the χ_1 and χ_2 values produced by incorporation of B repeat units into the molecular chain should be attributed to packing of the dendrons, which is less compact in syndiotactic and heterotactic systems than in isotactic ones. However, the hydrogen-bonding network (Figure 4b) is preserved in all cases. Consideration of all the data recorded from the simulations of the 13 B-containing heterotactic models allows one to propose a right-handed helix with averaged backbone dihedral angles of $\chi_1 = (-171.3 \pm 2.4)°$ and $\chi_2 = (-64.2 \pm 1.6)°$. The characteristic helical parameters of an idealized system that adopts such a conformation are 3.03 repeat units per turn, 0.79 Å internal radius, and 2.09 Å rise per repeat unit. These results clearly reflect that the helical conformation predicted for isotactic **PG2** is close to that obtained for heterotactic models. The most notable difference between the conformations obtained for isotactic and heterotactic **PG2** is the number of residues per turn, which is higher for the latter. The larger number of residues per turn in the heterotactic models results in enlargement of the helix pitch and therefore a decrease in the compactness of the dendritic side groups with respect to the isotactic model. Differences in the packing of the dendrons are clearly evidenced in Figure 6a, which compares the equatorial projections of the two idealized helical conformations. Moreover, the helical conformation proposed for the heterotactic model is fully

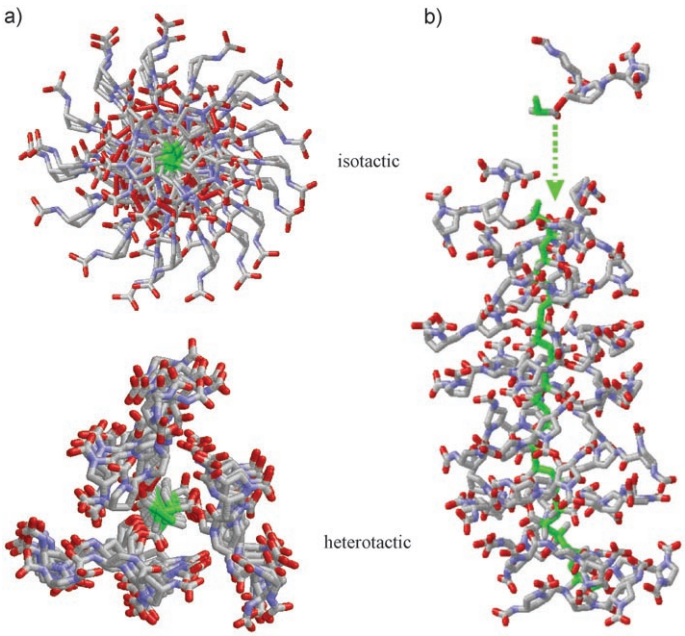

Figure 6. a) Equatorial projection of the right-handed helices proposed for isotactic and heterotactic **PG2**. b) Schematic showing helix formation of growing heterotactic **PG2** chain with incoming dendron. *tert*-Butyl groups and hydrogen atoms have been removed for clarity. The backbone is represented by a solid green line in all cases.

compatible with the growth of the polymer chain during the polymerization process. Thus, the low steric hindrance between the incoming dendron and the helix (Figure 6b) supports helix formation during polymerization.

To gain insight into the energetic stability of the different sequences, a simple energy analysis was performed on the last 50 snapshots recorded during the simulations. Specifically, we calculated the averaged internal energy of the **PG2** helix (E_{den}) and the potential energy of the whole simulated system (E_{den+s}), whereby the latter includes both the dendronized model molecule and the explicit solvent molecules. Relative values of E_{den} and E_{den+s} are included in Table 3. Although solute···solvent and solvent···solvent interactions alter the relative energy order derived from the analysis of the internal energy of the helix, the values of ΔE_{den} and ΔE_{den+s} lie within intervals of only 3.7 and 5.3 kcal mol^{-1} per repeat unit, respectively. Although such narrow intervals do not allow discrimination between the different models, they provide more evidence of both the significant stability of the helical conformation and its independence with respect to backbone tacticity.

Conclusion and Outlook

Attachment of compact, chiral second-generation dendrons with a low conformational flexibility to polymethacrylates forces the dendrons into tight register and thus not only makes the polymer highly rigid but also induces a conformation with a right-handed helical sense that is stable over a wide temperature range in both MeOH ($\varepsilon = 33$, protic) and THF ($\varepsilon = 6$, aprotic). Molecular dynamics simulations provided a right-handed helix model that is stable for isotactic, syndiotactic, and heterotactic **PG2**. Thus, backbone tacticity mainly affects the packing of the dendrons, which is less compact for syndiotactic and heterotactic **PG2** than for the isotactic system. Although the main trends of the secondary structure are not altered, the backbone tacticity modulates the characteristic helical parameters: the helix pitch and the number of r.u.s per turn of 6.33 Å and 3.03, respectively, for the heterotactic polymer decrease to 5.62 Å and 2.65 for the isotactic polymer. This allows the conclusion that helix formation during polymerization is mainly driven by dendron/dendron interaction and not by backbone tacticity. The backbone seems to be "decoupled" from the dendritic layer. The interdendron interaction, which is supported by interdendron hydrogen bonds, is strong enough to cope with any eventual structural constraints originating from backbone stereochemistry. This result differs from the findings of Okamoto and Nakano on trityl polymethacrylates, in which backbone tacticity is essential for the polymer to attain a helical conformation.[22] In their systems helical organization is believed to lead to an extended trityl-based chromophore, whereas in our case the chromophores appear to be more localized.

Because of the good availability of the monomer, **PG2** could, in principle, be easily prepared on a multigram scale and thus be used for further investigations such as formation of self-assembled hybrid structures with biological helices, as well as covalent decoration on the basis of selective addressability[27] of its peripheral protected primary and secondary amino groups.[28] Finally, with other diastereomers of **2a** at hand, an obvious next task to see whether not only right-handed but also left-handed helices can be obtained with the present concept.

Experimental Section

Materials: Dendrons **1a** and **2a** were synthesized according to our previous report.[15] THF was dried by refluxing over lithium aluminum hydride, and dichloromethane by distillation from CaH_2. Methacryloyl chloride (MAC) was freshly distilled before use. Other reagents and solvents were purchased in reagent grade and used without further purification. All reactions and polymerizations were run under a nitrogen atmosphere. Macherey-Nagel precoated TLC plates (silica gel 60 G/UV_{254}, 0.25 mm) were used for thin-layer chromatography (TLC) analysis, and separation on the plates was visualized by treatment with ethanolic ninhydrin solution (1%) and subsequently heating at ca. 200 °C. Silica gel 60 M (Macherey-Nagel, 0.04–0.063 mm, 230–400 mesh) was used as stationary phase for column chromatography. All samples were dried thoroughly under vacuum prior to analytical measurements to remove strongly adhering solvent molecules.

Characterization: All characterization was done with one and the same sample. ^{1}H and ^{13}C NMR spectra were recorded on Bruker AM 300 (^{1}H: 300 MHz, ^{13}C: 75 MHz) and AV 500 (^{1}H: 500 MHz, ^{13}C: 125 MHz) spectrometers at room temperature with $CDCl_3$ or CD_3OD as solvent, and chemical shifts are reported as δ values (ppm) relative to internal Me_4Si. Solid-state NMR measurements were kindly done in Prof. Beat Meier's group (ETH Zürich). ESI-MS and high-resolution MALDI-TOF MS analyses were performed by the MS service of the Laboratorium für Organische Chemie, ETH Zürich, on an IonSpec Ultra instrument. Optical rotations were measured on a Perkin-Elmer 241 polarimeter with a 1 dm cuvette. UV measurements were performed on a Varian Cary 100 Bio UV/Vis spectrophotometer equipped with a thermostatically regulated bath in a 1 mm quartz cell. Circular dichroism measurements were performed on a JASCO J-715 spectropolarimeter with a thermocontrolled 1 mm quartz cell (5 accumulations, continuous scanning mode, scanning speed 20 nm min^{-1}, data pitch: 1 nm, response: 1 s, band width: 5.0 nm). Gel permeation chromatography (GPC) was carried out on a PL-GPC 220 instrument with a 2× PL-Gel Mix-B LS column set (2×30 cm) equipped with refractive index (RI), viscosity, and light-scattering (LS; 15 and 90° angles) detectors, and LiBr (1 g L^{-1}) in DMF as eluent at 80 °C. Universal calibration was performed with poly(methyl methacrylate) standards in the range of $M_p = 2680$–$3\,900\,000$ (Polymer Laboratories Ltd, UK). Differential scanning calorimetry (DSC) measurements were performed on a DSC Q1000 differential scanning calorimeter from TA Instruments in the temperature range of −80 to +200 °C with a heating rate of 10 °C min^{-1}. Samples of total weight ranging between 3 and 10 mg were sealed in 40 μL aluminum pans, covered by a holed cap, and analyzed under a nitrogen atmosphere. The glass transition temperature T_g was determined in the second heating run.

Calculations: Quantum chemical calculations on **2c** were performed at the HF/3-21G,[23] HF/6–31G(d),[24] and B3LYP/6–31G(d)[25] levels with the Gaussian 03 program suite.[29] Atomistic MD simulations of isotactic, syndiotactic, and heterotactic models of **PG2** were performed with the NAMD program.[30] For NVT-MD in chloroform and methanol solutions, the simulated system was placed in the center of an orthorhombic simulation box filled with explicit solvent molecules. Chloroform was represented by the four-particle OPLS model,[31] while the all-atom model reported by Caldwell and Kollman was used for methanol.[32] In all cases **PG2** was simulated by considering explicitly all atoms of a 20 r.u. model molecule, which was blocked at the ends with methyl groups. The dimensions of the orthorhombic box for simulations in chloroform and methanol solutions were (99.31×99.31×115.00) and (105.65×105.65×115.25) Å^3, respectively, while the total number of particles considered explicitly was 35 496 (8267 chloroform molecules) and 115 888 (18 910 methanol molecules). The energy was calculated with the AMBER force field,[26] and all parameters required for **PG2** were taken from the AMBER libraries with the exception of the electrostatic ones. Atomic charges (see the Supporting Information) were explicitly developed by using a previously developed procedure.[33] For this purpose, the molecular electrostatic potential was calculated at the HF/6-31G(d) level for a model system constituted by 3 r.u.s. Atom-pair distance cutoffs were applied at 12.0 Å to compute the van der Waals interactions. The electrostatic interactions were computed by using the nontruncated electrostatic potential with Ewald summations.[34] The real-space term was determined by the van der Waals cut off (12.0 Å). Bond lengths involving hydrogen atoms were constrained by using the SHAKE algorithm[35] with a numerical integration step of 2 fs. Before the MD production series, the thermodynamic variables of the system were equilibrated. The energy of each system was initially minimized to relax conformational and structural tensions by using the conjugate gradient method for 5×10^3 steps. Next, the dendronized polymer was placed in a previously equilibrated solvent box. Different consecutive rounds of short MD runs were performed to equilibrate the variable thermodynamic magnitudes. First, solvent was thermally relaxed by three consecutives runs, while the dendronized polymer was kept frozen: 0.2 ns of NVT-MD at 500 K was used to homogeneously distribute the solvent in the box. Second, 0.15 ns of isothermal relaxation at 298 K was run. Finally, all atoms of the system were submitted to 0.25 ns of NVT-

MD at 298 K (thermal equilibration). Temperature was controlled by the weak coupling method, the Berendsen thermostat,[36] with a time constant for heat-bath coupling of 1 ps. The end of the thermal relaxation simulation was the starting point of the molecular simulations presented in this work. All simulations were performed at 298 K. The coordinates of all the production runs, which were between 6 and 50 ns long, were saved every 500 steps (1 ps intervals) for subsequent analysis.

Structural analyses: The conformational stability and conservation of the helix when the **PG2** model changes from isotactic to syndiotactic and heterotactic was measured by calculating the evolution of the backbone root mean square deviation (RMSD) through the simulation relative to the idealized helix proposed for the heterotactic model and the root mean square fluctuation (RMSF) of individual repeat units averaged over the whole simulation. To obtain the helix parameters for idealized models, the backbone dihedral angles were averaged with consideration of the 18 central repeat units, that is, the dihedral angles of the repeat units located at the end were omitted because of the frying. The end-to-end distance was obtained by measuring the distance between the carbon atoms of the blocking methyl groups of each recorded microstructure.

Syntheses

General procedure for reduction of esters to alcohols (A): $LiBH_4$ (5 mmol) in THF was added dropwise to a solution of dendron ester (1 mmol) in dry THF (25 mL) at −10 °C. The mixture was stirred for 3 h and then overnight at room temperature. Ethyl acetate (10 mL) was added to quench the reaction. Evaporation of the solvents in vacuo at room temperature gave a residue that was dissolved in dichloromethane. It was washed successively with saturated $NaHCO_3$ and brine. All aqueous phases were extracted with dichloromethane three times, and the combined organic phase was dried over $MgSO_4$. After filtration, the solvent was evaporated in vacuo. Purification by column chromatography afforded the colorless alcohol.

General procedure for the synthesis of macromonomers (B): MAC (2.4 mmol) in THF (20 mL) was dropped into a solution of the dendron-*n*-alcohol (2.0 mmol), triethylamine (10.0 mmol), and 4-dimethylaminopyridine (0.1 g) in dry THF (80 mL) at 0 °C. The mixture was stirred for 2 h and then overnight at room temperature. Evaporation of the solvents in vacuo at room temperature gave a residue, which was dissolved in dichloromethane. It was washed successively with saturated $NaHCO_3$ and brine. All aqueous phases were extracted with dichloromethane three times, and the combined organic phase was dried over $MgSO_4$. After filtration, the solvent was evaporated in vacuo at room temperature. Purification by column chromatography afforded a colorless foam, which was kept at −20 °C before use.

General procedure for thermally induced radical polymerization of macromonomers (C): A solution of macromonomer (0.3–0.5 g) in DMF (0.4 mL) in a Schlenk tube was degassed by several freeze–pump–thaw cycles and then kept at 60 °C with stirring for a predetermined time. Polymerization was stopped by cooling, and the polymer was dissolved in dichloromethane and purified by column chromatography (silica gel, dichloromethane eluent).

(2*S*,4*S*)-1-*tert*-Butoxycarbonyl-4-(*tert*-butoxycarbonylamino)-2-pyrrolidinylmethanol (1b): General procedure A with **1a** (17.0 g, 49.4 mmol) and $LiBH_4$ (250 mmol) yielded **1b** as a colorless foam (14.4 g, 92 %). ^{1}H NMR (500 MHz, $CDCl_3$): δ = 1.42 and 1.44 (2 s, 18 H; CH_3), 1.52–1.55 (m, 1 H; CH_2), 2.33–2.36 (m, 1 H; CH_2), 3.04–3.10 (m, 1 H; CH_2), 3.53–3.57 (m, 1 H; CH_2OH), 3.70–3.74 (m, 1 H; CH_2), 3.80–3.88 (m, H, CH_2OH), 3.93 (s, H, CH), 4.10–4.12 ppm (m, 1 H; CH); ^{13}C NMR (125 MHz, $CDCl_3$): δ = 28.21, 28.35, 28.37, 28.52, 34.40, 34.80, 35.04, 48.58, 53.62, 53.74, 59.00, 66.20, 79.47, 79.54, 80.38, 80.49, 155.32, 156.32 ppm; MS (ESI): *m*/*z*: 317.1 $[M+H]^+$, 339.1 $[M+Na]^+$.

(2*S*,4*S*)-1-Boc-4-(*tert*-Butoxycarbonylamino)-2-(methacryloyloxymethyl)-pyrrolidine (1c): General procedure B with **1b** (5.0 g, 15.8 mmol) and MAC (1.98 g, 18.9 mmol) afforded **1c** as a colorless solid (5.8 g, 95 %). ^{1}H NMR (500 MHz, $CDCl_3$): δ = 1.45 and 1.46 (2 s, 9 H; CH_3), 1.70–1.75 (m, 1 H; CH_2), 1.96 (s, 3 H; CH_3), 2.40–2.45 (m, 1 H; CH_2), 3.10–3.12 (m, 1 H; CH_2), 3.82–3.88 (m, 1 H; CH), 4.10–4.15 (m, 2 H; CH + CH_2), 4.31–4.41 (m, 2 H; CH + CH_2), 5.60 (s, 1 H; CH), 6.12 ppm (s, 1 H; CH); ^{13}C NMR (125 MHz, $CDCl_3$): δ = 18.38, 28.32, 28.36, 28.46, 34.16, 35.34, 49.25, 52.64, 53.16, 54.88, 64.97, 79.67, 79.97, 125.93, 136.01, 154.32, 155.23, 167.19 ppm; MS (ESI): *m*/*z*: 407.2210 $[M+Na]^+$.

(2*S*,4*S*)-1-[(2*S*,4*S*)-1-(*tert*-Butoxycarbonyl)-4-(*tert*-butoxycarbonylamino)-pyrrolidine-2-carbonyl]-4-[(2*S*,4*S*)-1-(*tert*-butoxycarbonyl)-4-(*tert*-butoxycarbonylamino)pyrrolidine-2-carbonylamino]-2-pyrrolidinylmethanol (2b): General procedure A with ester **2a** (4.0 g, 5.20 mmol) and $LiBH_4$ in NMP (13 mL) yielded alcohol **2b** as a colorless solid (3.5 g, 91 %). ^{1}H NMR (500 MHz, $CDCl_3$): δ = 1.39, 1.41, and 1.43 (3 s, 36 H; CH_3), 1.74–1.84 (m, 2 H; CH_2), 2.24–2.28 (m, 2 H; CH_2), 3.33–3.38 (m, 2 H; CH_2), 3.30–3.64 (m, 6 H; CH_2), 3.76–4.05 (m, 2 H; CH), 4.20–4.32 ppm (m, 4 H; CH); ^{13}C NMR (125 MHz, $CDCl_3$): δ = 28.29, 28.38, 28.41, 28.46, 34.12, 34.44, 35.73, 36.02, 36.13, 49.88, 50.12, 50.35, 50.81, 53.52, 54.11, 54.83, 56.29, 56.97, 57.12, 59.87, 79.32, 80.22, 80.80, 81.08, 153.30, 154.27, 155.44, 171.90, 173.09 ppm; MS (MALDI): *m*/*z*: 763.4224 $[M+Na]^+$, 779.3968 $[M+K]^+$.

(2*S*,4*S*)-1-[(2*S*,4*S*)-1-(*tert*-Butoxycarbonyl)-4-(*tert*-butoxycarbonylamino)-pyrrolidine-2-carbonyl]-4-[(2*S*,4*S*)-1-(*tert*-butoxycarbonyl)-4-(*tert*-butoxycarbonyl amino)pyrrolidine-2-carbonylamino]-2-methacryloyloxymethyl-pyrrolidine (2c): General procedure B with **2b** (2.0 g, 2.70 mmol) and MAC (0.34 g) afforded **2c** as a colorless solid (2.0 g, 92 %). ^{1}H NMR (500 MHz, $CDCl_3$): δ = 1.35, 1.36, 1.38, and 1.39 (4 s, 36 H; CH_3), 1.71–1.74 (m, 2 H; CH_2), 1.90 (s, 3 H; CH_3), 2.24–2.35 (m, 4 H; CH_2), 3.26–3.58 (m, 5 H; CH_2), 4.10–4.46 (m, 7 H; CH + CH_2), 5.54 (s, 1 H; CH_2), 6.06 ppm (s, 1 H; CH_2); ^{13}C NMR (125 MHz, $CDCl_3$): δ = 17.52, 18.31, 28.21, 28.32, 28.39, 31.49, 32.23, 35.83, 36.74, 49.00, 49.20, 50.10, 52.90, 53.76, 54.45, 55.01, 55.30, 56.83, 59.31, 63.01, 63.44, 79.16, 79.27, 80.10, 80.18, 81.00, 126.03, 126.18, 135.95, 153.27, 154.25, 155.36, 156.14, 167.14, 172.30, 172.53 ppm; MS (MALDI): *m*/*z*: 831.4468 $[M+Na]^+$, 847.4242 $[M+K]^+$.

Poly[(2*S*,4*S*)-1-*tert*-butoxycarbonyl-4-(*tert*-butoxycarbonylamino)-2-(methacryloyloxymethyl)pyrrolidine] (PG1): General procedure C with monomer **1c** (0.50 g) and DMF (0.5 mL) yielded **PG1** as a colorless solid (0.42 g, 84 %). ^{1}H NMR (500 MHz, $CDCl_3$): δ = 0.93 (br, 3 H; CH_3), 1.41 (br, 18 H; CH_3), 1.76 (br, 1 H; CH_2), 2.36 (br, 1 H; CH_2), 2.94 (br, 1 H; CH_2), 4.03 ppm (br, 5 H; CH + CH_2).

Poly[(2*S*,4*S*)-1-[(2*S*,4*S*)-1-(*tert*-butoxycarbonyl)-4-(*tert*-butoxycarbonyl-amino)pyrrolidine-2-carbonyl]-4-[(2*S*,4*S*)-1-(*tert*-butoxycarbonyl)-4-(*tert*-butoxycarbonylamino)pyrrolidine-2-carbonylamino]-2-methacryloyloxy-methylpyrrolidine] (PG2): General procedure C with monomer **2c** (0.50 g) and DMF (0.5 mL) yielded **PG2** as a colorless solid (0.32 g, 64 %). ^{13}C NMR (75 MHz, solid state): δ = 29.0, 36.6, 45.9, 50.9, 56.9, 79.8, 155.0, 174.4 ppm.

Poly{[(2*S*,4*S*)-1-[(2*S*,4*S*)-4-aminopyrrolidine-2-carbonyl)-4-[(2*S*,4*S*)-4-aminopyrrolidine-2-carboxamido]pyrrolidin-2-yl)methyl methacrylate] (*de*-PG2). Trifluoroacetic acid (2 g) was added to a solution of **PG2** (200 mg) in dichloromethane (15 mL) at 0 °C, and the mixture was stirred at room temperature for 5 h. Excess MeOH was then added to quench the reaction. After evaporation of solvents, slightly yellowish polymer was obtained quantitatively. ^{1}H NMR (500 MHz, [D$_6$]DMSO, 120 °C): δ = 0.89 (br; CH_3), 1.01 (br; CH_3), 1.28 (br; CH_3), 1.92 (br; CH_2), 3.29 (br; CH_2), 3.83 (br; CH), 4.26 ppm (br; CH).

Acknowledgements

We thank Prof. R. J. M. Nolte (RU Nijmegen), as well as Prof. W. Suter and Prof. P. Walde (ETH Zürich) for helpful discussion. Prof. A. Vasella and Prof. F. Diederich (ETH Zürich) are thanked for kindly providing access to their instruments. M. Colussi and D. Sutter are thanked for GPC and solution NMR measurements, respectively. Prof. B. Meier and his group (ETH Zürich) are thanked for the solid-state NMR measurement. This work was financially supported by the National Science Foundation of China (Nos. 20374047 & 20574062), the Swiss National Science Foundation (No. 200021-113690), MCYT and FEDER (No. MAT2006-04029), as well as ETH research Grant TH-35/05-1. Computer resources were generously provided by the Barcelona Supercomputer Center (BSC) and the "Centre de Supercomputació de Catalunya" (CESCA).

D.Z. and F.R.R. are thankful for financial support from the "Ramón y Cajal" and FPU programs, respectively, of the Spanish MEC. We cordially thank the two reviewers for their helpful comments and kind suggestions.

[1] a) Y. Okamoto, T. Nakano, *Chem. Rev.* **1994**, *94*, 349–372; b) T. Nakano, Y. Okamoto, *Chem. Rev.* **2001**, *101*, 4013–4038; c) J. J. L. M. Cornelissen, A. E. Rowan, R. J. M. Nolte, N. A. J. M. Sommerdijk, *Chem. Rev.* **2001**, *101*, 4039–4070; d) M. M. Green, K.-S. Cheon, S.-Y. Yang, J.-W. Park, S. Swansburg, W. Liu, *Acc. Chem. Res.* **2001**, *34*, 672–680; e) E. Yashima, K. Maeda, T. Nishimura, *Chem. Eur. J.* **2004**, *10*, 42–51. J.G. Rudick, V. Percec, *New J. Chem.* **2007**, *31*, 1083–1096; f) A. R. A. Palmans, E. W. Meijer, *Angew. Chem.* **2007**, *119*, 9106–9126; *Angew. Chem. Int. Ed.* **2007**, *46*, 8948–8968; g) E. Yashima, K. Maeda, *Macromolecules* **2008**, *41*, 3–12.

[2] a) S.-I. Sakurai, K. Okoshi, J. Kumaki, E. Yashima, *J. Am. Chem. Soc.* **2006**, *128*, 5650–5651; b) J.-L. Zhou, X.-F. Chen, X.-H. Fan, C.-X. Lu, Q.-F. Zhou, *J. Polym. Sci., Part A Polym. Chem.* **2006**, *44*, 6047–6054; c) K. K. L. Cheuk, J. W. Y. Lam, B.-S. Li, Y. Xie, B.-Z. Tang, *Macromolecules* **2007**, *40*, 2633–2642; d) H. Zhao, F. Sanda, T. Masuda, *J. Polym. Sci. Part A Polym. Chem.* **2007**, *45*, 1691–1698; e) T. Fujii, M. Shiotsuki, Y. Inai, F. Sanda, T. Masuda, *Macromolecules* **2007**, *40*, 7079–7088; f) M. Goh, M. Kyotani, K. Akagi, *J. Am. Chem. Soc.* **2007**, *129*, 8519–8527.

[3] a) S. Mayer, R. Zentel, *Prog. Polym. Sci.* **2001**, *26*, 1973–2013; b) M. M. Green, N. C. Peterson, T. Sato, A. Teramoto, R. Cook, S. Lifson, *Science* **1995**, *268*, 1860–1865; c) M. M. Green, S. Zanella, H. Gu, T. Sato, G. Gottarelli, S. K. Jha, G. P. Spada, A. M. Schoevaars, B. L. Feringa, A. Teramoto, *J. Am. Chem. Soc.* **1998**, *120*, 9810–9817; d) M. M. Green, J. W. Park, T. Sato, A. Teramoto, S. Lifson, R. L. B. Selinger, J. V. Selinger, *Angew. Chem.* **1999**, *111*, 3328–3345; *Angew. Chem. Int. Ed.* **1999**, *38*, 3138–3154; e) D. Pijper, B. L. Feringa, *Angew. Chem.* **2007**, *119*, 3767–3770; *Angew. Chem. Int. Ed.* **2007**, *46*, 3693–3696.

[4] a) J. R. Koe, M. Fujiki, H. Nakashima, M. Motonaga, *Chem. Commun.* **2000**, 389–390; b) T. Sanji, K. Takase, H. Sakurai, *J. Am. Chem. Soc.* **2001**, *123*, 12690–12691; c) M. Fujiki, *Macromol. Rapid Commun.* **2001**, *22*, 539–563; d) A. Ohira, S.-Y. Kim, M. Fujiki, Y. Kawakami, M. Naito, G. Kwak, A. Saxena, *Chem. Commun.* **2006**, 2705–2707.

[5] a) A. Goodwin, B. M. Novak, *Macromolecules* **1994**, *27*, 5520–5522; b) G. Tian, Y. Lu, B. M. Novak, *J. Am. Chem. Soc.* **2004**, *126*, 4082–4083; c) H.-Z. Tang, B. M. Novak, J. He, P. L. Polavarapu, *Angew. Chem.* **2005**, *117*, 7464; *Angew. Chem. Int. Ed.* **2005**, *44*, 7298 –7301.

[6] a) T. Nakano, Y. Shikisai, Y. Okamoto, *Polym. J.* **1996**, *28*, 51–60; b) T. Nakano, Y. Okamoto, *Macromolecules* **1999**, *32*, 2391–2393; c) C. A. Müller, T. Hoffart, M. Holbach, M. Reggelin, *Macromolecules* **2005**, *38*, 5375 –5380.

[7] a) J. J. L. M. Cornelissen, M. Fischer, N. A. J. M. Sommerdijk, R. J. M. Nolte, *Science* **1998**, *280*, 1427–1430; b) J. J. L. M. Cornelissen, J. J. J. M. Donners, R. de Gelder, W. S. Graswinckel, G. A. Metselaar, A. E. Rowan, N. A. J. M. Sommerdijk, R. J. M. Nolte, *Science* **2001**, *293*, 676–680; c) F. Takei, H. Hayashi, K. Onitsuka, N. Kobayashi, S. Takahashi, *Angew. Chem.* **2001**, *113*, 4216–4218; *Angew. Chem. Int. Ed.* **2001**, *40*, 4092–4094; d) J. J. L. M. Cornelissen, N. A. J. M. Sommerdijk, R. J. M. Nolte, *Macromol. Chem. Phys.* **2002**, *203*, 1625–1630; e) S. J. Wezenberg, G. A. Metselaar, A. E. Rowan, J. J. L. M. Cornelissen, D. Seebach, R. J. M. Nolte, *Chem. Eur. J.* **2006**, *12*, 2778–2786; f) E. Schwartz, H. J. Kitto, R. de Gelder, R. J. M. Nolte, A. E. Rowan, J. J. L. M. Cornelissen, *J. Mater. Chem.* **2007**, *17*, 1876–1884; g) Y. Hase, Y. Mitsutsuji, M. Ishikawa, K. Maeda, K. Okoshi, E. Yashima, *Chem. Asian J.* **2007**, *2*, 755–763; h) H. Onouchi, K. Okoshi, T. Kajitani, S.-I. Sakurai, K. Nagai, J. Kumaki, K. Onitsuka, E. Yashima, *J. Am. Chem. Soc.* **2008**, *130*, 229–236.

[8] a) N. Hoshikawa, Y. Hotta, Y. Okamoto, *J. Am. Chem. Soc.* **2003**, *125*, 12380–12381; b) A. K. M. F. Azam, M. Kamigaito, Y. Okamoto, *J. Polym. Sci. Part A, Polym. Chem.* **2007**, *45*, 1304–1315; c) G. M. Miyake, W. R. Mariott, E. Y.-X. Chen, *J. Am. Chem. Soc.* **2007**, *129*, 6724–6725.

[9] a) A. D. Schlüter, J. P. Rabe, *Angew. Chem.* **2000**, *112*, 860–880; *Angew. Chem. Int. Ed.* **2000**, *39*, 864–883; b) A. Zhang, L. Shu, Z. Bo, A. D. Schlüter, *Macromol. Chem. Phys.* **2003**, *204*, 328–339; c) A. Zhang, *Prog. Chem.* **2005**, *17*, 157–171; d) H. Frauenrath, *Prog. Polym. Sci.* **2005**, *30*, 325–384; e) A. D. Schlüter, *Top. Curr. Chem.* **2005**, *245*, 151–191.

[10] H. Zhao, F. Sanda, T. Masuda, *Macromol. Chem. Phys.* **2006**, *207*, 1921–1926.

[11] a) V. Percec, J. G. Rudick, M. Peterca, M. Wagner, M. Obata, C. M. Mitchell, W.-D. Cho, V. S. K. Balagurusamy, Paul A. Heiney, *J. Am. Chem. Soc.* **2005**, *127*, 15257–15264; b) V. Percec, J. G. Rudick, M. Peterca, S. R. Staley, M. Wagner, M. Obata, C. M. Mitchell, W.-D. Cho, V. S. K. Balagurusamy, J. N. Lowe, M. Glodde, O. Weichold, K. J. Chung, N. Ghionni, S. N. Magonov, P. A. Heiney, *Chem. Eur. J.* **2006**, *12*, 5731–5746; c) V. Percec, E. Aqad, M. Peterca, J. G. Rudick, L. Lemon, J. C. Ronda, B. B. De, P. A. Heiney, E. W. Meijer, *J. Am. Chem. Soc.* **2006**, *128*, 16365–16372.

[12] W. Zhang, M. Shiotsuki, T. Masuda, *Macromol. Rapid Commun.* **2007**, *28*, 1115–1121.

[13] Y. Suzuki, M. Shiotsuki, F. Sanda, T. Masuda, *Macromolecules* **2007**, *40*, 1864–1867.

[14] A simple measure of the compactness of dendrons is the number of atoms between the branching points, which for **PG2** are denoted as BP in Scheme 1. Note that for nonsymmetric dendrons the branches can consist of many different atoms. For the dendronized polymer **PG2** the numbers of atoms between BPs are 2,4 (see Scheme 1). 3,3: a) S. M. Grayson, J. M. J. Fréchet, *Macromolecules* **2001**, *34*, 6542–6544; 3,3: b) M. Malkoch, A. Carlmark, A. Woldegiorgis, A. Hult, E. E. Malmström, *Macromolecules* **2004**, *37*, 322–329; 7,7: c) A. Zhang, L. Okrasa, T. Pakula, A. D. Schlüter, *J. Am. Chem. Soc.* **2004**, *126*, 6658; 8,8: d) E. Kasëmi, W. Zhuang, J. P. Rabe, K. Fischer, M. Schmidt, M. Colussi, H. Keul, D. Yi, H. Cölfen, A. D. Schlüter, *J. Am. Chem. Soc.* **2006**, *128*, 5091–5099.

[15] A. Zhang, A. D. Schlüter, *Chem. Asian J.* **2007**, *2*, 1540–1548.

[16] High purity is a prerequisite for spontaneous polymerization. It is reasonable to assume that the polymerization is initiated by some inadvertently formed radical: A. Zhang, B. Zhang, E. Wächtersbach, M. Schmidt, A. D. Schlüter, *Chem. Eur. J.* **2003**, *9*, 6083.

[17] For peptidic dendronized polymers, see: a) G. Draheim, H. Ritter, *Macromol. Chem. Phys.* **1995**, *196*, 2211–2222; b) M. Niggemann, H. Ritter, *Acta Polym.* **1996**, *47*, 351–356; c) M. Niggemann, H. Ritter, *J. Macromol. Sci. Pure Appl. Chem.* **1997**, *A34*, 1325–1338; d) A. Bilibin, I. Zorin, S. Saratovsky, I. Moukhina, G. Egorova, N. Girbasova, *Macromol. Symp.* **2003**, *199*, 197–208; e) N. Girbasova, V. Aseyev, S. Saratovsky, I. Moukhina, H. Tenhu, A. Bilibin, *Macromol. Chem. Phys.* **2003**, *204*, 2258–2264; f) M. A. Zhuravel, N. E. Davis, S. T. Nguyen, I. Koltover, *J. Am. Chem. Soc.* **2004**, *126*, 9882–9883; g) A. Luebbert, T. Q. Nguyen, F. Sun, S. S. Sheiko, H.-A. Klok, *Macromolecules* **2005**, *38*, 2064–2071; h) C. Lee, J. M. J. Frechet, *Macromolecules* **2006**, *39*, 476–481.

[18] The NMR spectrum of **PG2** in [D_6]DMF at 25 °C was very similar to that in $CDCl_3$, while a rather well-resolved spectrum was obtained in [D_6]DMF at 80 °C (See Figure S1 in the Supporting Information).

[19] K. Hatada, T. Kitayama, K. Ute, *Prog. Polym. Sci.* **1988**, *13*, 189–276.

[20] R. Al-Hellani, A. D. Schlüter, *Helv. Chim. Acta* **2006**, *89*, 2745–2763.

[21] J. F. G. A. Jansen, H. W. I. Peerlings, E. M. M. de Brabander-van den Berg, E. W. Meijer, *Angew. Chem.* **1995**, *107*, 1321–1324; *Angew. Chem. Int. Ed. Engl.* **1995**, *34*, 1206–1209.

[22] From the work of Okamoto and Nakano on trityl polymethacrylates with extended chromophores associated with the trityl groups, it is known that polymethacrylates must have high backbone tacticity in order to adopt a helical conformation: a) T. Nakano, M. Mori, Y. Okamoto, *Macromolecules* **1993**, *26*, 867–868; b) T. Nakano, Y. Okamoto, *Macromol. Rapid Commun.* **2000**, *21*, 603–612.

[23] J. S. Binkley, J. A. Pople, W. J. Hehre, *J. Am. Chem. Soc.* **1980**, *102*, 939–947.
[24] P. C. Hariharan, J. A. Pople, *Theor. Chim. Acta* **1973**, *28*, 213–222.
[25] a) A. D. Becke, *J. Chem. Phys.* **1993**, *98*, 1372–1377; b) C. T. Lee, W. Yang, R. G. Parr, *Phys. Rev. B* **1988**, *37*, 785–789.
[26] W. D. Cornell, P. Cieplak, C. I. Bayly, I. R. Gould, K. M. Merz, D. M. Ferguson, D. C. Spellmeyer, T. Fox, J. W. Caldwell, P. A. Kollman, *J. Am. Chem. Soc.* **1995**, *117*, 5179–5197.
[27] R. Al-Hellani, A. D. Schlüter, *Macromolecules* **2006**, *39*, 8943–8951.
[28] a) S. C. Nigam, A. Mann, M. Taddei, C.-G. Wermuth, *Synth. Commun.* **1989**, *19*, 3139–3142; b) K. Ravinder, A. V. Reddy, K. C. Mahesh, M. Narasimhulu, Y. Venkateswarlu, *Synth. Commun.* **2007**, *37*, 281–287.
[29] Gaussian 03, Revision B.02, M. J. Frisch, G. W. Trucks, H. B. Schlegel, G. E. Scuseria, M. A. Robb, J. R. Cheeseman, J. A. Montgomery, Jr., T. Vreven, K. N. Kudin, J. C. Burant, J. M. Millam, S. S. Iyengar, J. Tomasi, V. Barone, B. Mennucci, M. Cossi, G. Scalmani, N. Rega, G. A. Petersson, H. Nakatsuji, M. Hada, M. Ehara, K. Toyota, R. Fukuda, J. Hasegawa, M. Ishida, T. Nakajima, Y. Honda, O. Kitao, H. Nakai, M. Klene, X. Li, J. E. Knox, H. P. Hratchian, J. B. Cross, V. Bakken, C. Adamo, J. Jaramillo, R. Gomperts, R. E. Stratmann, O. Yazyev, A. J. Austin, R. Cammi, C. Pomelli, J. W. Ochterski, P. Y. Ayala, K. Morokuma, G. A. Voth, P. Salvador, J. J. Dannenberg, V. G. Zakrzewski, S. Dapprich, A. D. Daniels, M. C. Strain, O. Farkas, D. K. Malick, A. D. Rabuck, K. Raghavachari, J. B. Foresman, J. V. Ortiz, Q. Cui, A. G. Baboul, S. Clifford, J. Cioslowski, B. B. Stefanov, G. Liu, A. Liashenko, P. Piskorz, I. Komaromi, R. L. Martin, D. J. Fox, T. Keith, M. A. Al-Laham, C. Y. Peng, A. Nanayakkara, M. Challacombe, P. M. W. Gill, B. Johnson, W. Chen, M. W. Wong, C. Gonzalez, J. A. Pople, Gaussian, Inc., Wallingford CT, **2004**.
[30] J. C. Phillips, R. Braun, W. Wang, J. Gumbart, E. Tajkhorshid, E. Villa, C. Chipot, R. D. Skeel, L. Kale, K. Schulten, *J. Comput. Chem.* **2005**, *26*, 1781–1802.
[31] W. L. Jorgensen, J. Chandrasekhar, J. D. Madura, R. W. Impey, M. L. Klein, *J. Chem. Phys.* **1983**, *79*, 926–935.
[32] J. W. Caldwell, P. A. Kollman, *J. Phys. Chem.* **1995**, *99*, 6208–6219.
[33] C. Alemán, F. J. Luque, M. Orozco, *J. Comput. Aided Mol. Design* **1993**, *7*, 721–742.
[34] T. Darden, D. York, L. Pedersen, *J. Chem. Phys.* **1993**, *98*, 10089–10092.
[35] J. P. Ryckaert, G. Ciccotti, H. J. C. Berendsen, *J. Comput. Phys.* **1977**, *23*, 327–341.
[36] H. J. C. Berendsen, J. P. M. Postma, W. F. van Gunsteren, A. Dinola, J. R. Haak, *J. Chem. Phys.* **1984**, *81*, 3684–3690.

Received: February 21, 2008
Revised: April 30, 2008
Published online: July 4, 2008

